


## Gravitational form factors of light nuclei: Impulse approximation

Fangcheng He<sup>✉\*</sup> and Ismail Zahed<sup>†</sup>

*Center for Nuclear Theory, Department of Physics and Astronomy, Stony Brook University, Stony Brook, New York 11794–3800, USA*

 (Received 29 October 2023; revised 19 March 2024; accepted 1 April 2024; published 22 April 2024)

The gravitational form factors of light nuclei are evaluated up to momenta of the order of the nucleon mass, using the impulse approximation. The nucleon gravitational form factors are reduced nonrelativistically, and used to derive the gravitational form factors of light nuclei. The deuteron gravitational form factors are analysed using the Reid soft core potential. The helium-4 gravitational form factors are assessed using the  $K$ -harmonics method, and compared to those following from a mean-field approximation with a Woods-Saxon potential. The importance of removing the center of mass motion for the ensuing form factors is emphasized. The mass radii of these light nuclei are extracted and compared to their charge radii counterparts. The details of their pressure and shear distributions are discussed.

DOI: [10.1103/PhysRevC.109.045209](https://doi.org/10.1103/PhysRevC.109.045209)

### I. INTRODUCTION

The gravitational form factors of the nucleon carry important information on its mass distribution, most of which is carried by constituent gluons. Recently, threshold photoproduction of charmonium at Jefferson Laboratory (JLab) [1] has opened the possibility of measuring the gluonic component of the nucleon gravitational form factors. The high statistics results reported by the E12-007 collaboration [2], suggest smaller mass radii for the proton in comparison to its electromagnetic radius.

Threshold electromagnetic production of charmonium off light nuclei could open the possibility of understanding the nuclear effects on the gravitational form factors. The nucleus is a collection of nucleons (protons and neutrons) bound by strong quantum chromodynamics (QCD) interactions. Most of what is known about nuclei has been gleaned using electromagnetic probes at intermediate energies [3], where the nucleons appear as rigid but extended bodies exchanging mesons, albeit mostly pions [4] (and references therein). The disparity between the fundamental and unconfined degrees of QCD (quarks and gluons) and the observed but confined degrees of freedom (mesons and nucleons) call for novel probes. The ultimate goal is to understand the composition of the nucleons, and how the nuclear interactions emerge in a nucleus.

The difficult character of the strong nuclear interaction, has required the use of approximate models to account for the motion of the nucleons in a bound nucleus. Mean field models of which the shell model is the ultimate realization, have proven successful in interpreting many aspects of low and intermediate nuclear physics. However, much is still needed for a theory to be sufficiently accurate and predictive. For this

reason, the study of simpler nuclei such as deuterium, triton, and helium-3,4 should prove useful for the study of novel probes, such as the one provided by the energy-momentum tensor (EMT).

The simplest nuclear system is of course the deuteron. Its binding energy (2.225 MeV), charge radius (2.13 fm), and magnetic moment (0.857 in Bohr magnetons) are well established, which strongly constrain the pair nucleon-nucleon interaction [5]. The deuteron large size and weak binding suggests that the nuclear interaction is due to single pion exchange between almost on-shell nucleons. The deuteron is a diffuse nucleus.

The purpose of this work is to provide the starting framework for the nuclear effect on the deuteron EMT. We will derive in detail its gravitational form factors using the impulse approximation. The results are readily extended to spherically symmetric and light nuclei such as helium-4, which is the prototype nucleus per excellence, given that its binding energy per particle is close to the saturation one.

For completeness, we note that the gravitational  $D$ -form factors for nuclei were initially discussed using a liquid drop model in [6], relativistic nuclear potentials in [7], nuclear structure [8–13], and more recently the generalized Skyrme model in [14]. Also, the spatial densities and forces in the deuteron were discussed in [15] using the light cone convolution model. An estimate of the mass radius of helium-4 was suggested recently using  $\phi$ -meson photoproduction [16].

The outline of this paper is as follows. In Sec. II we briefly review the chief aspects of the deuteron  $S, D$  contributions using Reid soft core potential. In Sec. III we summarize the relevant aspects of the nucleon gravitational  $A, B, C = \frac{1}{4} D$  form factors. To use them for low and intermediate energies up to the nucleon mass scale, we explicitly present their non-relativistic expansions. In Sec. IV we derive the deuteron gravitational form factors in the impulse approximation, and in leading order in the recoil momentum of the spectator nucleon. In Sec. V we extend our results to helium-4 using both

\*fangcheng.he@stonybrook.edu

†ismail.zahed@stonybrook.edu

the  $K$ -harmonics method and the mean-field approximation with a Woods-Saxon potential. The importance of removing the spurious center of mass motion, while addressing the form factors of light nuclei is emphasized. In Sec. VI we detail the extraction of the mass radii from the pertinent EMT form factors. Our conclusions are in Sec. VII. In Appendix A, we compare our deuteron and helium-4 charge form factors versus the existing data. In Appendix B, we briefly recall the pressure and shear force used.

## II. DEUTERON STATE

The deuteron with the tiny 2.2 MeV binding is a loosely bound light nucleus composed of almost quasifree proton plus neutron held together by a long range pion-exchange interaction. In the nonrelativistic approximation, the deuteron

wave function is a mixture of  ${}^3S_1 + {}^3D_1$ ,

$$\Phi_m(r) = \left( \frac{u}{r} + \frac{1}{\sqrt{8}} \frac{w}{r} S_{12} \right) \frac{\chi_m}{\sqrt{4\pi}} \quad (1)$$

with the deuteron quadrupole operator

$$S_{12} = 6S \cdot \hat{r} S \cdot \hat{r} - 2S^2 = 6Q^{ij} \hat{r}^i \hat{r}^j \quad (2)$$

with total spin  $\vec{S}$ , where  $Q^{ij}$  is the quadrupole operator  $Q^{ij} = \frac{1}{2}(S^i S^j + S^j S^i) - \frac{2}{3}\delta^{ij}$ . The reduced radial wave functions  $u, w$  are normalized,

$$\int_0^\infty dr (u^2 + w^2) = 1. \quad (3)$$

The coupled  $u, w$  reduced radial components  ${}^3S_1$  and  ${}^3D_1$  of the deuteron wave function will be sought using a central and tensor interaction [17]

$$\begin{aligned} u'' + \frac{m}{\hbar^2}(-E - V_C(r))u - \sqrt{8} \frac{m}{\hbar^2} V_T w &= 0, \\ w'' + \frac{m}{\hbar^2} \left( -E - V_C(r) - \frac{6\hbar^2}{mr^2} + 2V_T(r) + 3V_{LS}(r) \right) w - \sqrt{8} \frac{m}{\hbar^2} V_T u &= 0 \end{aligned} \quad (4)$$

with the Reid soft core potential  $V_R = V_C + V_T S_{12} + V_{LS} L \cdot S$ ,

$$\begin{aligned} V_C &= -h \frac{e^{-x}}{x} + 105.468 \text{ (MeV)} \frac{e^{-2x}}{x} - 3187.8 \text{ (MeV)} \frac{e^{-4x}}{x} + 9924.3 \text{ (MeV)} \frac{e^{-6x}}{x}, \\ V_T &= -h \left( \left( \frac{1}{x} + \frac{3}{x^2} + \frac{3}{x^3} \right) e^{-x} - \left( \frac{12}{x^2} + \frac{3}{x^3} \right) e^{-4x} \right) + 351.77 \text{ (MeV)} \frac{e^{-4x}}{x} - 1673.5 \text{ (MeV)} \frac{e^{-6x}}{x}, \\ V_{LS} &= 708.91 \text{ (MeV)} \frac{e^{-4x}}{x} - 2713.1 \text{ (MeV)} \frac{e^{-6x}}{x}. \end{aligned} \quad (5)$$

Here,  $x = \mu r$  is the pion range fixed by  $\mu = 0.7 \text{ fm}^{-1}$ , as illustrated in Fig. 1 (top). Also  $h = 10.463 \text{ MeV}$  and  $\hbar^2/m$  is assumed to be  $41.47 \text{ MeV fm}^2$  with  $m$  the twice reduced mass of proton and neutron. The numerical  $S$ - and  $D$ -wave functions solution to the coupled equations (5) and valid for  $x < 10.01$ , are shown in Fig 1 (bottom). For  $x > 10.01$ , the explicit solutions are [17]

$$\begin{aligned} u(r) &= 0.87758 e^{-\alpha \mu r}, \\ w(r) &= 0.0023 e^{-\alpha \mu r} \left( 1 + \frac{3}{\alpha \mu r} + \frac{3}{(\alpha \mu r)^2} \right) \end{aligned} \quad (6)$$

with  $\alpha = (mE_D)^{1/2}/(\mu\hbar)$ . The deuteron solution in Fig. 1 (bottom) carries binding energy  $E_D = 2.2246 \text{ MeV}$ , and a quadrupole moment

$$Q_D^E = \frac{1}{4} \int d^3r |\Phi_1(r)|^2 (3z^2 - r^2) \approx 0.31 \text{ fm}^2 \quad (7)$$

in the  $z$  direction and the maximally stretches spin state. The deuteron is mostly cigar-shaped. This deformation amounts to  $p_D = 6.53\%$ , the percentage of admixture of  $D$  state in the deuteron [17].

## III. NUCLEON EMT

The standard decomposition of EMT form factor in a nucleon state is [18–20]

$$T_N^{\mu\nu}(p_2, p_1) = \langle p_2 | T^{\mu\nu}(0) | p_1 \rangle = \bar{u}(p_2) \left( A(k) \gamma^{(\mu} \bar{P}^{\nu)} + B(k) \frac{i\bar{P}^{(\mu} \sigma^{\nu)\alpha} k_\alpha}{2m_N} + C(k) \frac{k^\mu k^\nu - \eta^{\mu\nu} k^2}{m_N} \right) u(p_1) \quad (8)$$

with  $a^{(\mu} b^{\nu)} = \frac{1}{2}(a^\mu b^\nu + a^\nu b^\mu)$ ,  $k^2 = (p_2 - p_1)^2 = t$ ,  $\bar{P} = (p_1 + p_2)/2$ , and the normalization  $\bar{u}u = 1$ . Equation (8) is conserved and trace full. Note that in other conventions, the  $C$ -form factor is also referred to by  $D(k) = 4C(k)$ .

The gluonic gravitational form factors (GFFs) have been analyzed both analytically and numerically, and more recently extracted empirically with overall good agreements. For the numerical analyses below, we will use a triple

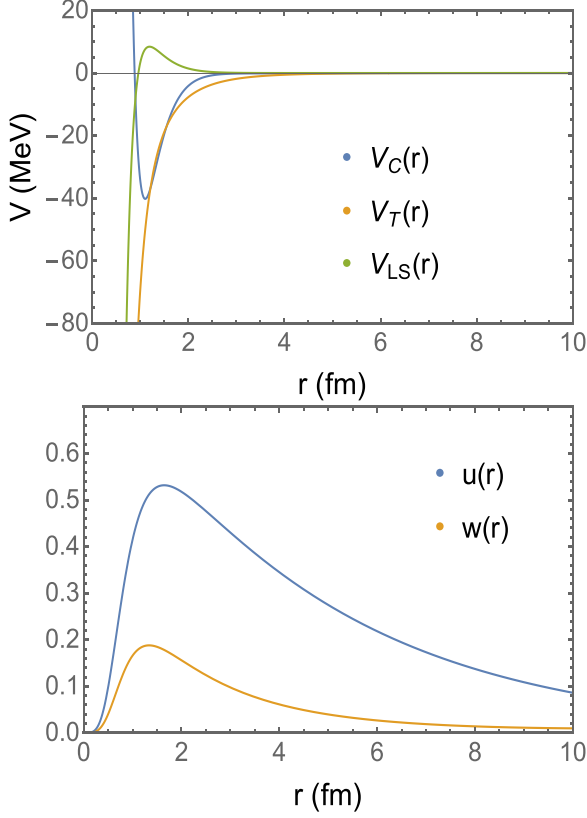


FIG. 1. Top: Reid soft core potentials  $V_{C,T,LS}$ ; bottom: deuteron  $S, D$  wave functions in Eq. (4).

parametrization of the holographic results for the gluon GFFs, and a dipole parametrization for the lattice quark GFFs with  $k^2 = -Q^2$  space-like,

$$A_g(k) = \frac{A_g(0)}{\left(1 + \frac{Q^2}{m_{TT,g}^2}\right)^3}, \quad A_q(k) = \frac{A_q(0)}{\left(1 + \frac{Q^2}{m_{TT,q}^2}\right)^2},$$

$$C_g(k) = \frac{\frac{1}{4}D_g(0)}{\left(1 + \frac{Q^2}{m_{SS,g}^2}\right)^3}, \quad C_q(k) = \frac{\frac{1}{4}D_q(0)}{\left(1 + \frac{Q^2}{m_{SS,q}^2}\right)^2} \quad (9)$$

with  $m_{TT,g} = 1.612$  GeV,  $m_{TT,q} = 1.477(44)$  GeV,  $m_{SS,g} = 0.963$  GeV,  $m_{SS,q} = 0.81(14)$  GeV,  $A_g(0) = 0.430$ ,  $A_q(0) = 0.510(25)$ ,  $D_g(0) = -1.275$ , and  $D_q(0) = -1.30(49)$ . The parameters of the gluon GFFs are from the holographic model [22], in overall agreement with those recently reported by the E12-007 collaboration [2]. The quark GFFs are obtained by recent lattice results in [21], as illustrated in Fig. 2. To fix the sum rule  $A_q(0) + A_g(0) = 1$ , we set  $A_q(0) = 0.57$ , which is slightly larger than the lattice results. The remaining EMT form factor  $B$  is null in dual gravity [22], and is very small in unpolarized lattice calculations [21] and global analysis [23].

Although, the holographic EMT form factors are given in terms of hypergeometric functions [22], Eq. (9) provides a good approximation for a wide range of momenta. They are in agreement with the hard scattering rules asymptotically. We will not consider the additional  $\bar{C}_{q,g}$  form factors as they

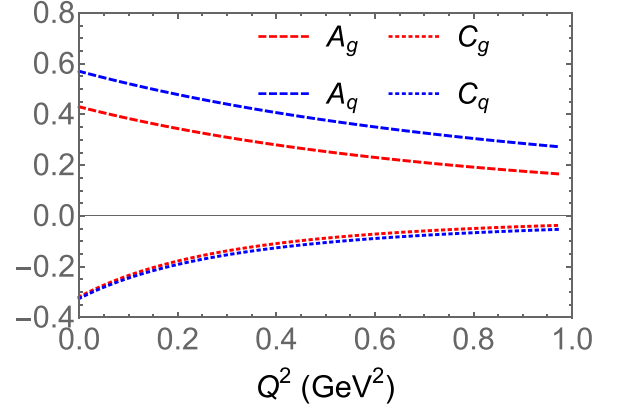


FIG. 2. Nucleon GFFs:  $A_q, C_q$  (quarks) are from the recent lattice results [21], and  $A_g, C_g$  (gluons) are from the holographic model [22].

are absent in the holographic construction, and add to zero in physical observables. Alternative discussions to some of these form factors can be found in [24–29].

In this work, we assume that the nucleons in the deuteron are quasifree particle since the binding energy is very small. For on-shell nucleons, we can use the Gordon identity to rewrite Eq. (8) as Eq. (10), which is more convenient for the non-relativistic reduction. More specifically, we have

$$T_N^{\mu\nu}(p_2, p_1) = \bar{u}(p_2) \left( A(k) \frac{\bar{P}^\mu \bar{P}^\nu}{m_N} + B(k) \frac{i\bar{P}^{(\mu} \sigma^{\nu)\alpha} k_\alpha}{2m_N} + C(k) \frac{k^\mu k^\nu - \eta^{\mu\nu} k^2}{m_N} \right) u(p_1). \quad (10)$$

To probe the EMT in the deuteron at low and intermediate momentum transfers, we will use a nonrelativistic reduction, with the assumption that it holds for  $k/m_N$  of about 1. The justification for this assumption can only be made *a posteriori*, by comparing to possibly future diffractive experiments. We recall that a similar assumption works reasonably well for the electromagnetic probes in the deuteron, at the nucleon mass scale [4]. With this in mind, the nonrelativistic reduction of Eq. (10) reads

$$T_N^{00}(k) = \left( A(k) m_N + \left( \frac{1}{8}A(k) - \frac{1}{4}B(k) + C(k) \right) \frac{\vec{k}^2}{m_N} \right) + \left( \frac{1}{2}A(k) + B(k) \right) \frac{(\sigma \times ik) \cdot P}{2m_N} + \mathcal{O}\left( \frac{\vec{k}^3}{m_N^2}, \frac{\vec{P}^2}{m_N} \right),$$

$$T_N^{0j}(k) = (A(k) + B(k)) \frac{(\sigma \times ik)^j}{4} + A(k) P^j + \mathcal{O}\left( \frac{\vec{k}^3}{m_N^2}, \frac{\vec{P}^2}{m_N} \right),$$

$$T_N^{jl}(k) = (A(k) + B(k)) \frac{(\sigma \times ik)^{jP^l}}{2m_N} + C(k) \frac{k^l k^j - \delta^{jl} \vec{k}^2}{m_N} + \mathcal{O}\left( \frac{\vec{k}^3}{m_N^2}, \frac{\vec{P}^2}{m_N} \right), \quad (11)$$

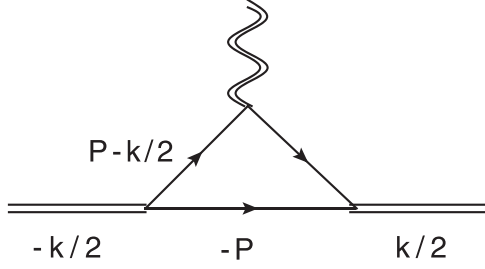


FIG. 3. A graviton through  $T^{\mu\nu}(k)$ , striking a nucleon in a deuteron with a recoiling spectator of momentum  $-P$ .

where  $P^j$  is the momentum of spectator shown in Fig. 3 and only terms linear in  $P^j$  are retained. This additional assumption is justified in the analysis of the EMT of the deuteron to follow. Indeed, the higher order terms in the expansion when evaluating in a deuteron state, are controlled by the binding energy  $E_D = 2.225$  MeV which is small,

$$\frac{\langle \vec{P}^2 \rangle}{m_N^2} \approx \frac{E_D}{m_N} \approx 10^{-3}.$$

With this in mind, and dropping the  $\mathcal{O}$  notations for convenience, Eq. (11) yields

$$\begin{aligned} T_N^{00}(k) &= T_M(k) + T_{SP}(k) \frac{(\sigma \times ik) \cdot P}{2m_N^2}, \\ T_N^{0j}(k) &= T_S(k) \frac{(\sigma \times ik)^j}{4m_N} + A(k)P^j, \\ T_N^{jl}(k) &= T_S(k) \frac{(\sigma \times ik)^{jP^l}}{2m_N^2} + C_M(k) \frac{k^j k^l - \delta^{jl} \vec{k}^2}{m_N^2}. \end{aligned} \quad (12)$$

For simplicity, we use the notation  $T_M(k)$ ,  $T_S(k)$ ,  $T_{SP}(k)$  to represent the contributions in Eq. (11) for mass, spin, and spin-recoil. They can be related to form factor  $A(k)$ ,  $B(k)$ , and  $C(k)$  through

$$\begin{aligned} T_M(k) &= A(k)m_N + \left( \frac{1}{8}A(k) - \frac{1}{4}B(k) + C(k) \right) \frac{\vec{k}^2}{m_N}, \\ T_S(k) &= m_N (A(k) + B(k)), \\ T_{SP}(k) &= m_N \left( \frac{1}{2}A(k) + B(k) \right), \\ C_M(k) &= m_N C(k). \end{aligned} \quad (13)$$

Since  $T^{00}$  and  $T^{0j}$  are related to the nucleon energy and spin, the factors  $T_M$ ,  $T_S$  represent the form factor of momentum fraction and angular momentum in the nucleon.

#### IV. DEUTERON EMT IN THE IMPULSE APPROXIMATION

In the first approximation, we can treat the proton and neutron in the deuteron as quasifree. In the impulse approximation, the EMT are the expectation values of Eq. (11) in the deuteron state. Since the EMT is isoscalar, the contributions

of the proton and neutron add equally:

$$\begin{aligned} &\left\langle +\frac{k}{2}m' \left| T_N^{00}(k) \right| -\frac{k}{2}m \right\rangle \\ &= 2T_M(k) \left\langle +\frac{k}{2}m' \left| \mathbf{1} \right| -\frac{k}{2}m \right\rangle \\ &\quad + 2T_{SP}(k) \left\langle +\frac{k}{2}m' \left| \frac{P \cdot (S \times ik)}{2m_N^2} \right| -\frac{k}{2}m \right\rangle, \\ &\left\langle +\frac{k}{2}m' \left| T_N^{0j}(k) \right| -\frac{k}{2}m \right\rangle \\ &= 2T_S(k) \left\langle +\frac{k}{2}m' \left| \frac{(S \times ik)^j}{4m_N} \right| -\frac{k}{2}m \right\rangle \\ &\quad + 2m_N A(k) \left\langle +\frac{k}{2}m' \left| \frac{P^j}{m_N} \right| -\frac{k}{2}m \right\rangle, \\ &\left\langle +\frac{k}{2}m' \left| T_N^{jl}(k) \right| -\frac{k}{2}m \right\rangle \\ &= 2T_S(k) \left\langle +\frac{k}{2}m' \left| \frac{(S \times ik)^{jP^l}}{2m_N^2} \right| -\frac{k}{2}m \right\rangle \\ &\quad + 2C_M(k) \frac{k^j k^l - \delta^{jl} \vec{k}^2}{m_N^2} \left\langle +\frac{k}{2}m' \left| \mathbf{1} \right| -\frac{k}{2}m \right\rangle. \end{aligned} \quad (14)$$

Here,  $m, m'$  refer to the azimuthal quantum numbers in Eq. (1) (not to be confused with the reduced mass). The matrix elements in the deuteron state can be simplified using symmetry arguments, and the conservation of the EMT. Their physical interpretation is best in the Breit (brick-wall) frame as illustrated in Fig. 3 with  $k^0 = 0$  and  $\vec{k} \cdot \vec{P} = 0$ .

The simplest matrix elements to evaluate do not involve the total momentum  $P$ , they will be evaluated first, followed by single and double total momenta. For the latter, we will rely on a wave function prescription to avoid issues of hermiticity.

#### A. Matrix element of $\mathbf{1}$

The details of the matrix element of  $\mathbf{1}$  will be provided in full to show how all matrix elements are evaluated. More specifically and following the kinematics depicted in Fig. 3, the matrix element can be defined as [30]

$$\begin{aligned} \left\langle +\frac{k}{2}m' \left| \mathbf{1} \right| -\frac{k}{2}m \right\rangle &= \int d^3P \Phi_m^\dagger \left( P + \frac{k}{4} \right) \mathbf{1} \Phi_m \left( P - \frac{k}{4} \right) \\ &= \int d^3r e^{\frac{i}{2}k \cdot r} \varphi_m^\dagger(r) \mathbf{1} \varphi_m(r), \end{aligned} \quad (15)$$

where we used the wave packet form for the deuteron in-out states

$$\Phi_m \left( P \pm \frac{k}{4} \right) = \int d^3r e^{-i(P \pm \frac{1}{4}k) \cdot r} \varphi_m(r). \quad (16)$$

Inserting Eq. (1) into Eq. (15) gives

$$\begin{aligned} \left\langle +\frac{k}{2}m' \left| \mathbf{1} \right| -\frac{k}{2}m \right\rangle &= C_E(k) \delta_{mm'} - 2C_Q(k) \langle m' | (S \cdot \hat{k})^2 | m \rangle \\ &\quad - \frac{1}{3} S^2 |m\rangle \end{aligned} \quad (17)$$

with the deuteron total spin and angular momentum

$$\vec{S} = \frac{1}{2}(\vec{\sigma}_p + \vec{\sigma}_n) = \vec{\sigma}, \quad \vec{L} = \vec{L}_p + \vec{L}_n = \vec{r} \times \vec{P}, \quad (18)$$

and the form factors

$$C_E(k) = \int_0^\infty dr (u^2 + w^2) j_0\left(\frac{kr}{2}\right),$$

$$C_Q(k) = \frac{3}{\sqrt{2}} \int_0^\infty dr \left(uw - \frac{w^2}{2\sqrt{2}}\right) j_2\left(\frac{kr}{2}\right). \quad (19)$$

The deviation from spherical symmetry follows from the  $D$ -wave content of the deuteron wave function. We note that  $C_E(0) = 1$  as expected from the deuteron charge normalization, and that near the forward limit

$$C_Q(k) \approx \frac{Q_D^E}{4} \vec{k}^2 \quad (20)$$

with the quadrupole moment  $Q_D^E \approx 0.31 \text{ fm}^2$ .

### B. Matrix element of $(S \times ik)^j$

Similarly, the spin contribution can be obtained by symmetry using the Wigner-Eckart theorem

$$\left\langle +\frac{k}{2}m' \left| (S \times ik)^j \right| -\frac{k}{2}m \right\rangle$$

$$= \int d^3r e^{\frac{i}{2}kr} \varphi_m^\dagger(r) (S \times ik)^j \varphi_m(r)$$

$$= C_S(k) \langle m' | (S \times ik)^j | m \rangle \quad (21)$$

with the result

$$C_S(k) = \int_0^\infty dr j_0\left(\frac{kr}{2}\right) \left(u^2 - \frac{w^2}{2}\right)$$

$$+ \frac{1}{\sqrt{2}} \int_0^\infty dr j_2\left(\frac{kr}{2}\right) \left(wu + \frac{w^2}{\sqrt{2}}\right) \quad (22)$$

or by direct computation, by specializing to  $i = 2$ ,  $m = 1$ , and  $m' = 0$ , and choosing  $k = k\hat{z}$ . In the forward limit

$$C_S(0) = C_I(0) - 4C_P(0) = 1 - \frac{3}{2}p_D = 1 - \frac{3}{2}6.53\% \quad (23)$$

with  $C_P(0)$  given in Eq. (29) below, and  $p_D = 6.53\%$  the percentage of  $D$  admixture in the deuteron.

### C. Matrix element of $P^j$

The first recoil contribution  $P^j$  to the energy momentum tensor can be obtained as follows:

$$\left\langle +\frac{k}{2}m' \left| P^j \right| -\frac{k}{2}m \right\rangle$$

$$t^{jl} = -\frac{1}{4} \int d^3r e^{\frac{i}{2}kr} (\partial^j \varphi_m^\dagger(r) (\vec{S} \times \vec{k})^l \varphi_m(r) - \varphi_m^\dagger(r) (\vec{S} \times \vec{k})^l \partial^j \varphi_m(r)) + (l \leftrightarrow j)$$

$$= - \int d^3r e^{\frac{i}{2}kr} \left( \frac{\sqrt{2}r (u'w - w'u) - w^2 + 2\sqrt{2}uw}{16r^3} \right) (\hat{r}^j (\vec{S} \times \vec{k})^l S_{12} - \hat{r}^j S_{12} (\vec{S} \times \vec{k})^l)$$

$$- \int d^3r e^{\frac{i}{2}kr} \frac{3wu}{4\sqrt{8}r^3} ((\sigma_1^j \sigma_2 \cdot \hat{r} + \sigma_2^j \sigma_1 \cdot \hat{r}) (\vec{S} \times \vec{k})^l - (\vec{S} \times \vec{k})^l (\sigma_1^j \sigma_2 \cdot \hat{r} + \sigma_2^j \sigma_1 \cdot \hat{r}))$$

$$= \int d^3P \Phi_{m'}^\dagger \left( P + \frac{1}{4}k \right) P^j \Phi_m \left( P - \frac{1}{4}k \right)$$

$$= \frac{i}{2} \int d^3r e^{\frac{i}{2}kr} \left( \partial_j \varphi_{m'}^\dagger(r) \varphi_m(r) - \varphi_{m'}^\dagger(r) \partial_j \varphi_m(r) \right). \quad (24)$$

Inserting the explicit derivative of the deuteron wave function

$$\partial_j \varphi_m(r) = \left( \left( \frac{u'(r)}{r} - \frac{u(r)}{r^2} - \frac{w(r)}{\sqrt{2}r^2} \right) \hat{r}^j \right.$$

$$+ \left. \left( \frac{w'(r)}{\sqrt{8}r} - \frac{3w(r)}{\sqrt{8}r^2} \right) S_{12}(\hat{r}) \hat{r}^j \right.$$

$$+ \left. \frac{3w(r)}{\sqrt{8}r} \left( \frac{\sigma_1^j \sigma_2 \cdot \hat{r} + \sigma_2^j \sigma_1 \cdot \hat{r}}{r} \right) \right) \chi_m \quad (25)$$

in Eq. (24), and using the identities

$$\frac{j_1\left(\frac{kr}{2}\right)}{kr} = \frac{j_0\left(\frac{kr}{2}\right) + j_2\left(\frac{kr}{2}\right)}{6},$$

$$\int d^3r e^{i\frac{\vec{k}\cdot\vec{r}}{2}} \hat{r}^j = 4\pi \int r^2 dr j_1\left(\frac{kr}{2}\right) i\hat{k}^j, \quad (26)$$

we can finally reduce Eq. (24) to

$$\left\langle +\frac{k}{2}m' \left| P^j \right| -\frac{k}{2}m \right\rangle = C_P(k) \langle m' | (S \times ik)^j | m \rangle \quad (27)$$

with

$$C_P(k) = \int dr \frac{3w^2}{8} \left( j_0\left(\frac{kr}{2}\right) + j_2\left(\frac{kr}{2}\right) \right). \quad (28)$$

Its forward contribution is readily tied to the admixture of  $D$  state in the deuteron

$$C_P(0) = \frac{3}{8} p_D = \frac{3}{8} 6.53\%. \quad (29)$$

Equation (27) is manifestly transverse to the direction of momentum  $k$ . The Breit frame projection through  $P^i \rightarrow \vec{P}^i$  as in Eq. (32) below, leaves it unchanged.

### D. Matrix element of $(S \times ik)^j P^l$

This matrix element can be obtained by evaluating first

$$t^{jl} = \left\langle +\frac{k}{2}m' \left| \frac{1}{2} \left( P^j (\vec{S} \times i\vec{k})^l + P^l (\vec{S} \times i\vec{k})^j \right) \right| -\frac{k}{2}m \right\rangle. \quad (30)$$

More specifically, the reduction of Eq. (30) follows the same reasoning as above with

$$\begin{aligned}
& - \int d^3r e^{\frac{i}{2}k \cdot r} \frac{3w^2}{32r^3} ((\sigma_1^j \sigma_2 \cdot \hat{r} + \sigma_2^j \sigma_1 \cdot \hat{r})(\vec{S} \times \vec{k})^l S_{12} - S_{12}(\vec{S} \times \vec{k})^l (\sigma_1^j \sigma_2 \cdot \hat{r} + \sigma_2^j \sigma_1 \cdot \hat{r})) + (l \leftrightarrow j) \\
= & \frac{1}{k} \int dr \left( \frac{\sqrt{2}r(u'w - w'u) - w^2 + 2\sqrt{2}uw}{16r} \right) \left[ \left( \frac{10}{kr} j_2\left(\frac{kr}{2}\right) - j_1\left(\frac{kr}{2}\right) \right) \right. \\
& \times \left( 24 \frac{k^j k^l}{\vec{k}^2} Q^{\alpha\beta} k_\alpha k_\beta - 12(Q^{j\beta} k_l k_\beta + Q^{l\beta} k_j k_\beta) \right) - \frac{48 j_2\left(\frac{kr}{2}\right)}{kr} (\delta^{jl} Q^{\alpha\beta} k_\alpha k_\beta - \vec{k}^2 Q^{jl}) \left. \right] \\
& + \frac{1}{k} \int dr \left( \frac{wu}{\sqrt{8}r} - \frac{w^2}{8r} \right) j_1\left(\frac{kr}{2}\right) (6\delta^{jl} Q^{\alpha\beta} k_\alpha k_\beta - 6\vec{k}^2 Q^{jl}) \\
& + \frac{1}{k} \int dr \frac{9w^2}{8r} j_1\left(\frac{kr}{2}\right) ((\vec{S} \times k)^l (\vec{S} \times k)^j + (\vec{S} \times k)^j (\vec{S} \times k)^l) \\
& + \frac{1}{k} \int dr \frac{3w^2}{2r} \frac{j_2\left(\frac{kr}{2}\right)}{kr} (4(\delta^{jl} \vec{k}^2 - k^l k^j) - 3(\vec{S} \times k)^l (\vec{S} \times k)^j - 3(\vec{S} \times k)^j (\vec{S} \times k)^l \\
& + 3(2\delta^{jl} Q^{\alpha\beta} k_\alpha k_\beta - Q^{j\beta} k_l k_\beta - Q^{l\beta} k_j k_\beta)). \tag{31}
\end{aligned}$$

The matrix element in Eq. (31) lacks manifest transversality, i.e.,  $k^l t^{jl} \neq 0$ . This is caused by the off-shell character of the struck nucleon which leads to the violation of the kinematic condition:  $\vec{k} \cdot \vec{P} \neq 0$  say in the Breit frame. To enforce the Breit frame condition  $\vec{k} \cdot \vec{P} = 0$  in the matrix elements, we will make the operator substitution

$$P^\mu \rightarrow \tilde{P}^\mu = P^\mu - \frac{(k \cdot P)}{k^2} k^\mu. \tag{32}$$

This replacement is carried out in the evaluation of the EMT nucleon matrix elements, rather than the evaluation of the wave function in Eq. (16), followed by the Breit frame substitution (32). This amounts to the projection

$$\tilde{t}^{jl} = t^{jl} - \frac{k^l t^{j\alpha} k^\alpha + k^j t^{l\alpha} k^\alpha}{k^2} + k^j k^l \frac{k^\alpha t^{\alpha\beta} k^\beta}{k^4} \tag{33}$$

when evaluating the matrix elements of the EMT in the deuteron state. The upshot of this substitution, is the manifest conservation of the the recoil corrections in the deuteron EMT,

$$\tilde{t}^{jl} = \frac{k^l k^j - \delta^{jl} \vec{k}^2}{2} D_0^{SP} + (k^j k^\alpha Q^{l\alpha} + k^l k^\alpha Q^{j\alpha} - \vec{k}^2 Q^{jl} - \delta^{jl} Q^{\alpha\beta} k_\alpha k_\beta) D_2^{SP} + (k^j k^l - \delta^{jl} \vec{k}^2) Q^{\alpha\beta} \hat{k}_\alpha \hat{k}_\beta D_3^{SP} \tag{34}$$

with

$$\begin{aligned}
D_0^{SP} &= - \int dr \frac{3w^2 j_1\left(\frac{kr}{2}\right)}{kr}, \\
D_2^{SP} &= + \int dr \frac{3krw(\sqrt{2}u + w)j_1\left(\frac{kr}{2}\right) - 6j_2\left(\frac{kr}{2}\right)(\sqrt{2}u(2w - rw') + w(\sqrt{2}ru' + 2w))}{2\vec{k}^2 r^2}, \\
D_3^{SP} &= - \int dr \frac{3(2j_2\left(\frac{kr}{2}\right)(2\sqrt{2}u(rw' - 2w) + w(5w - 2\sqrt{2}ru')) + krw(2\sqrt{2}u - w)j_1\left(\frac{kr}{2}\right))}{2\vec{k}^2 r^2}.
\end{aligned} \tag{35}$$

The net result is the matrix entry

$$\begin{aligned}
\left\langle +\frac{k}{2}m' \left| (S \times ik)^{(jP^l)} \right| -\frac{k}{2}m \right\rangle &= \frac{(k^j k^l - \delta^{jl} \vec{k}^2)}{2} D_0^{SP} \delta_{mm'} + \langle m' | (k^j k^\alpha Q^{l\alpha} + k^l k^\alpha Q^{j\alpha} - k^2 Q^{jl} - \delta^{jl} Q^{\alpha\beta} k_\alpha k_\beta) | m \rangle D_2^{SP} \\
&+ (k^j k^l - \delta^{jl} \vec{k}^2) \hat{k}_\alpha \hat{k}_\beta \langle m' | Q^{\alpha\beta} | m \rangle D_3^{SP}, \tag{36}
\end{aligned}$$

which is manifestly transverse, with all invariant form factors  $D_0^{SP}$ ,  $D_2^{SP}$ ,  $D_3^{SP}$  finite in the forward limit.

### E. Summary EMT in impulse approximation

In summary, the nonrelativistic contributions to the deuteron EMT in the impulse approximation and in linear order in the recoil momentum of the spectator nucleon, are given by

$$\begin{aligned}
T_D^{00}(k, m', m) &= 2T_M(k) \left( C_E(k) \delta_{mm'} - 2C_Q(k) \hat{k}_\alpha \hat{k}_\beta \langle m' | Q^{\alpha\beta} | m \rangle \right) \\
&\quad + 2T_{SP}(k) \left( -D_0^{SP}(k) \delta_{mm'} - (D_2^{SP}(k) + 2D_3^{SP}(k)) \hat{k}_\alpha \hat{k}_\beta \langle m' | Q^{\alpha\beta} | m \rangle \right) \frac{\vec{k}^2}{2m_N^2} \\
&= m_D A^D(k) \delta_{mm'} + Q^D(k) \frac{k_\alpha k_\beta}{2m_D} \langle m' | Q^{\alpha\beta} | m \rangle, \\
T_D^{0j}(k, m', m) &= 2T_S(k) C_S(k) \langle m' | \frac{(S \times ik)^j}{4m_N} | m \rangle + 2m_N A(k) C_P(k) \langle m' | \frac{(S \times ik)^j}{m_N} | m \rangle \\
&= J^D(k) \frac{\langle m' | (\vec{S} \times i\vec{k})^j | m \rangle}{2}, \\
T_D^{jl}(k, m', m) &= 2T_S(k) \left( \frac{(k^j k^l - \delta^{jl} \vec{k}^2)}{2} D_0^{SP}(k) \delta_{mm'} + (k^j k^l - \delta^{jl} \vec{k}^2) Q^{\alpha\beta} \hat{k}_\alpha \hat{k}_\beta D_3^{SP}(k) \right. \\
&\quad \left. + \langle m' | (k^j k^\alpha Q^{l\alpha} + k^l k^\alpha Q^{j\alpha} - \vec{k}^2 Q^{jl} - \delta^{jl} Q^{\alpha\beta} k_\alpha k_\beta) | m \rangle D_2^{SP}(k) \right) \frac{1}{2m_N^2} \\
&\quad + 2C_M(k) \frac{C_E(k) (k^j k^l - \delta^{jl} \vec{k}^2) \delta_{mm'} - 2C_Q(k) (k^j k^l - \delta^{jl} \vec{k}^2) \hat{k}_\alpha \hat{k}_\beta \langle m' | Q^{\alpha\beta} | m \rangle}{m_N^2} \\
&= D_0^D(k) \frac{k^j k^l - \delta^{jl} \vec{k}^2}{4m_D} \delta_{mm'} + D_3^D(k) \frac{(k^j k^l - \delta^{jl} \vec{k}^2) \hat{k}_\alpha \hat{k}_\beta \langle m' | Q^{\alpha\beta} | m \rangle}{4m_D} \\
&\quad + D_2^D(k) \frac{\langle m' | (k^j k^\alpha Q^{l\alpha} + k^l k^\alpha Q^{j\alpha} - \vec{k}^2 Q^{jl} - \delta^{jl} Q^{\alpha\beta} k_\alpha k_\beta) | m \rangle}{2m_D}. \tag{37}
\end{aligned}$$

Our conventions for the deuteron EMT invariant form factors, follow the general spin-1 conventions introduced in [31]. In the impulse approximation and to linear order in the recoil momentum of the spectator nucleon (in short hand notations), they are

$$\begin{aligned}
A^D &= \frac{2}{m_D} \left( T_M C_E - \frac{\vec{k}^2}{2m_N^2} T_{SP} D_0^{SP} \right), \\
Q^D &= -\frac{2m_D}{\vec{k}^2} \left( 4T_M C_Q + \frac{\vec{k}^2}{m_N^2} T_{SP} (D_2^{SP} + 2D_3^{SP}) \right), \\
J^D &= \frac{T_S C_S}{m_N} + 4A C_P, \\
D_0^D &= \frac{4m_D}{m_N^2} \left( \frac{1}{2} T_S D_0^{SP} + 2C_M C_E \right), \\
D_2^D &= \frac{2m_D}{m_N^2} T_S D_2^{SP}, \\
D_3^D &= \frac{4m_D}{m_N^2} (T_S D_3^{SP} - 4C_M C_Q) \tag{38}
\end{aligned}$$

with the deuteron quadrupole form factor

$$Q(k) = -\frac{4m_D^2}{\vec{k}^2} C_Q(k) \rightarrow Q_D \tag{39}$$

that reduces to the deuteron quadrupole moment in the forward direction.

The numerical results for low and intermediate momenta  $k \leq m_N$ , are shown in Fig. 4. Note that the quark and gluon contributions to  $D_0$  and  $D_3$  are comparable, since  $C_g(k)$  and  $C_q(k)$  are very similar in Eq. (9). In the impulse approximation, the spin averaged deuteron  $D$  value at the origin is  $D_0(0) = -10.43$ , which is to be compared to  $D_0(0) = -13.126$  in the Skyrme model [14], and  $D_0(0) = -24.33$  in the relativistic light cone convolution model [15].

For  $B(k) \approx 0$  and at low momenta  $k \ll m_N$ , we have

$$T_M(k) \approx T_S(k) \approx 2T_{SP}(k) \approx m_N A(k).$$

The deuteron invariant EMT form factors (38) simplify (short hand notation)

$$\begin{aligned}
A^D &\approx A(k) C_E, \\
Q^D &\approx -\frac{4m_D^2}{\vec{k}^2} A(k) C_Q - 2A(k) (D_2^{SP} + 2D_3^{SP}), \tag{40} \\
J^D &\approx A(k) (C_S + 4C_P)
\end{aligned}$$

for the mass  $A^D$ , quadrupole  $Q^D$ , and momentum  $J^D$ , respectively. For the deuteron  $D$  terms, we have (short hand

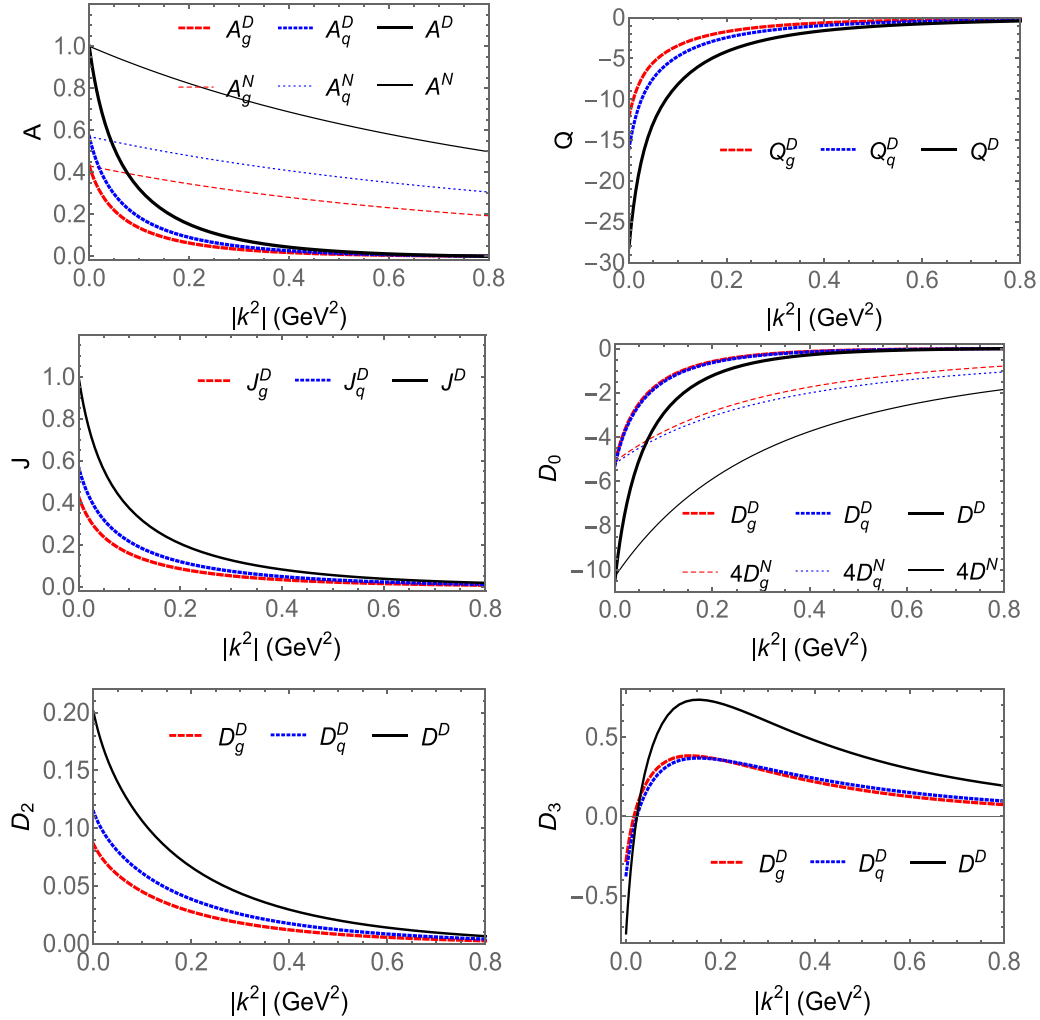


FIG. 4. The deuteron invariant EMT form factors (38) in the impulse approximation: gluon (red-dashed line), quark (blue-dotted line), and gluon+quark (black-solid line), compared to the nucleon  $A^N$  and  $D^N$  (thinner dashed, dotted, and solid lines).

notation)

$$\begin{aligned}
 D_0^D &\approx 4A(k)D_0^{SP} + 16C(k)C_E, \\
 D_2^D &\approx 4A(k)D_2^{SP}, \\
 D_3^D &\approx 8A(k)D_3^{SP} - 32C(k)C_Q
 \end{aligned}
 \quad (41)$$

for the standard tensor  $D_0^D$ , tensor spin-spin  $D_2^D$ , and tensor-quadrupole  $D_3^D$ , respectively.

The three deuteron  $D$ -form factors in the impulse approximation can be used to describe the spatial distributions of the pressure and shear force inside the deuteron as probed by a graviton or a graviton-like probes. Using the conventions for the pressure and shear introduced in [6], we show in Fig. 5 their distribution inside the deuteron. The formulas are put in Appendix B. We have separated the quark and gluon contributions, following their separation in the nucleon form factors (9). Here,  $p_{\{0,2,3\},\{g,q\}}$  refer to the pressure distributions carried by the quarks and gluons separately, and  $s_{\{0,2,3\},\{g,q\}}$  refer to the shear distributions carried by the quarks and gluons also separately. We note that the pressure distributions and shear forces obtained in this work satisfied the von Laue conditions mentioned in [31]. The sign of  $p_{0,g}$  changes

around  $r = 1.4$  fm, which is further than the one reported in the nucleon in [22]. Both  $p_{0,g}$  and  $s_{0,g}$  have longer tails in comparison to the nucleon.

## V. HELIUM-4 EMT IN THE IMPULSE APPROXIMATION

We will start with the simplest  $0^{++}$  helium-4 nucleus, a scalar particle both in spin and isospin. The ground state of helium-4 is composed of two protons and two neutrons in a purely  $S$  wave. Its  $0^{++}$  EMT is characterized by two invariant form factors [18]

$$\langle p_2 | T^{\mu\nu} | p_1 \rangle = \frac{P^\mu P^\nu}{m_\alpha} A^H(k) + \frac{1}{4m_\alpha} (k^\mu k^\nu - g^{\mu\nu} k^2) D^H(k). \quad (42)$$

In the impulse approximation, most of the EMT results for helium-4 can be inferred from those of the deuteron presented above with much simplifications. The same observations can be extended to the lighter  $0^{++}$  magic nuclei.



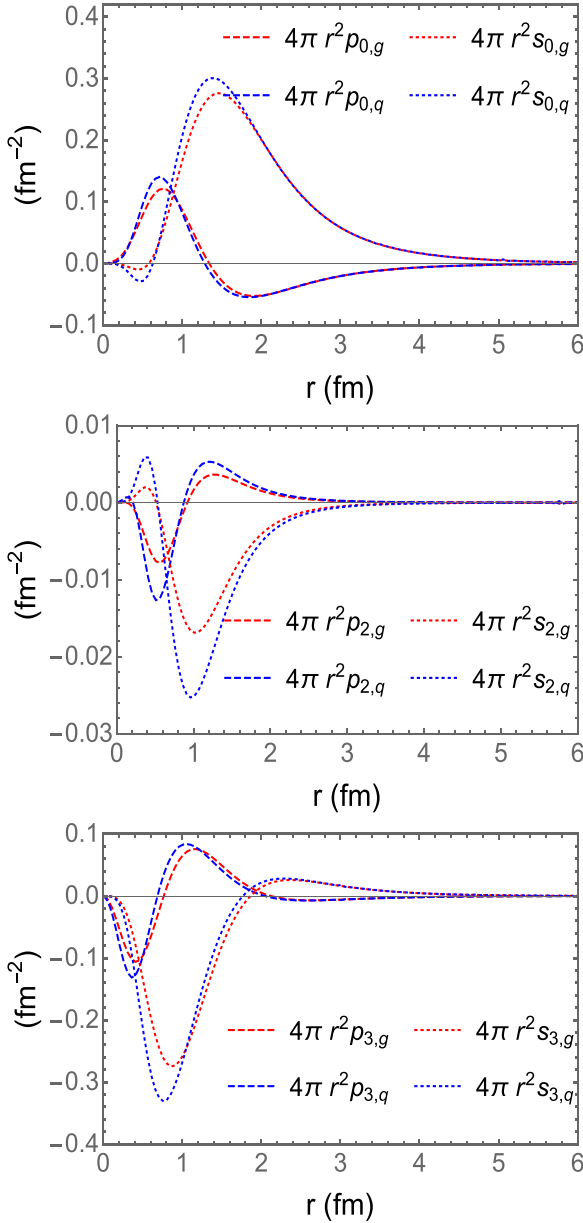


FIG. 5. The gluon and quark pressure  $p_{0,2,3}$  and shear  $s_{0,2,3}$  distributions inside the deuteron, in the impulse approximation.

### A. Helium-4 state

To construct the helium-4 state, we will use the  $K$ -harmonics method to factor out the spurious center of mass motion [32,33]. The method works well for few particle systems, when the multidimensional Schrodinger equation can be reduced to a one-dimensional hyper-radial distance times the lowest  $K$  harmonics.

The  $K$ -harmonics method becomes increasingly involved for heavier nuclei, where the mean-field single particle approximation is more appropriate. However, the removal of the spurious center of mass motion is more challenging in the mean-field approach. We will present both methods, when addressing helium-4 for comparison.

### 1. $K$ -harmonics method

The ground state of helium-4 ( $\alpha$  particle) is spin-isospin singlet, and reads

$$\Phi_H[1, \dots, 4] = \varphi[r_1, r_2, r_3, r_4] \mathbf{P}[\sigma(i), \tau(i)], \quad (43)$$

where  $\mathbf{P}[\ ]$  refers to the properly symmetrized spin-isospin wave function. In general, the ground state contains a smaller  $D$ -wave admixture [34], that we have ignored for simplicity.

To remove the spurious center of mass motion in Eq. (43) using the  $K$ -harmonics method, the pertinent Jacobi coordinates are [33]

$$\begin{aligned} \vec{\xi}_1 &= \frac{1}{\sqrt{2}}(\vec{r}_2 - \vec{r}_1), \\ \vec{\xi}_2 &= \frac{1}{\sqrt{6}}(\vec{r}_1 + \vec{r}_2 - 2\vec{r}_3), \\ \vec{\xi}_3 &= \frac{1}{2\sqrt{3}}(\vec{r}_1 + \vec{r}_2 + \vec{r}_3 - 3\vec{r}_4), \\ \vec{R}_C &= \frac{1}{4}(\vec{r}_1 + \vec{r}_2 + \vec{r}_3 + \vec{r}_4), \end{aligned} \quad (44)$$

the radial hyperdistance is

$$R^2 = \frac{1}{4} \sum_{i \neq j} (\vec{r}_i - \vec{r}_j)^2 = \vec{\xi}_1^2 + \vec{\xi}_2^2 + \vec{\xi}_3^2 \quad (45)$$

and the center of mass motion factors out of the four-particle kinetic contribution

$$\mathbb{K} = - \sum_{i=1}^4 \frac{\nabla_i^2}{2m_N} \rightarrow - \frac{1}{2m_N} \left( \frac{d^2}{dR^2} + \frac{8}{R} \frac{d}{dR} - \frac{K_N^2}{R^2} \right). \quad (46)$$

The hyperspherical harmonics (HHs) are the eigenstates of the grand-angular momentum [33]

$$K_N^2 \mathcal{Y}_{[K]}^{KLM_L}(\Omega_{\tilde{N}}) = (K(K + 3N - 2)) \mathcal{Y}_{[K]}^{KLM_L}(\Omega_{\tilde{N}}) \quad (47)$$

for atomic number  $A$  with  $N = A - 1$ . The  $\tilde{N} = 3N - 1$  angles are fixed by the hyperspherical symmetric Jacobi coordinates through

$$\begin{aligned} \xi_1 &= R \cos\theta (\sin\theta_1 \cos\phi_1, \sin\theta_1 \sin\phi_1, \cos\theta_1), \\ \xi_2 &= R \sin\theta \cos\phi (\sin\theta_2 \cos\phi_2, \sin\theta_2 \sin\phi_2, \cos\theta_2), \\ \xi_3 &= R \sin\theta \sin\phi (\sin\theta_3 \cos\phi_3, \sin\theta_3 \sin\phi_3, \cos\theta_3). \end{aligned} \quad (48)$$

They are valued as  $\theta_i \in [0, \pi]$ ,  $\phi_i \in [0, 2\pi]$ ,  $\theta \in [0, \frac{\pi}{2}]$ , and  $\phi \in [0, \frac{\pi}{2}]$  with the angular volumes

$$\begin{aligned} \Omega_9 &= \int_0^{\pi/2} d\phi \sin^2\phi \cos^2\phi \int_0^{\pi/2} d\theta \sin^5\theta \cos^2\theta \\ &\prod_{i=1}^3 \int_0^\pi d\theta_i \int_0^{2\pi} d\phi_i \sin\theta_i = \frac{32\pi^4}{105}. \end{aligned} \quad (49)$$

The specific form of the HHs follows by recoupling the individual angular momenta  $L_i$ . They are normalized as

$$\int d\Omega_{\tilde{N}} \mathcal{Y}_{[K]}^{KLM_L} * (\Omega_{\tilde{N}}) \mathcal{Y}_{[K']}^{K'L'M'_L}(\Omega_{\tilde{N}}) = \delta_{[K],[K']} \quad (50)$$

and their total number is

$$d_K = (2K + 3N - 2) \frac{(K + 3N - 3)!}{K!(3N - 2)!}. \quad (51)$$

For helium-4 with  $A = 4$  and  $N = 3$ , the  $K = 0$  HH has degeneracy  $d_0 = 1$ , and the  $K = 1$  HHs have degeneracy  $d_1 = 9$ . For  $K = 0$  case, the spin-isospin wave function can be written as [35]

$$\mathbf{P}[\sigma(i), \tau(i)] = \frac{\sqrt{105}}{8\pi^2} ([\sigma(1), \sigma(2)]_1 [\sigma(3), \sigma(4)]_1)_{00} ([\tau(1), \tau(2)]_0 [\tau(3), \tau(4)]_0)_{00} - ([\sigma(1), \sigma(2)]_0 [\sigma(3), \sigma(4)]_0)_{00} ([\tau(1), \tau(2)]_1 [\tau(3), \tau(4)]_1)_{00}. \quad (52)$$

Here,  $\sigma(i)$ ,  $\tau(i)$  refer to the spin-isospin of the  $i$ th nucleons. The subscripts refer to their recoupling to a total spin-isospin.

The general form of Eq. (43) in hyperspherical form modulo the spin factors is

$$\varphi_{[K]}(R) \mathcal{Y}_{[K]}^{KLM_L}(\Omega_{\mathbb{S}^3}) \quad (53)$$

with the  $S$ -wave solution for helium-4

$$\varphi_{[0]}(R) \mathcal{Y}_{[0]}^{000}(\Omega_{\mathbb{S}^3}) = \frac{\varphi(R)}{\sqrt{\Omega_9}}. \quad (54)$$

To eliminate the linear derivative in the hyperdistance in the Schrodinger equation, we will seek the radial wave function

$$\varphi(R) = \frac{u(R)}{R^4} \quad (55)$$

with the reduced wave function satisfying

$$u'' - \frac{12}{R^2}u - \frac{2m_N}{\hbar^2}(W(R) + V_C(R) - E)u = 0 \quad (56)$$

subject to the normalization

$$\int_0^\infty dR |u(R)|^2 = 1. \quad (57)$$

A large centrifugation emerges following the reduction to the hyperdistance. Here,  $W(R)$  is the projection of the pair potential  $V(r_{ij})$  on the  $K = 0$  harmonic, which can be obtained through [35]

$$W(R) = \frac{1}{\Omega_9} \int d\Omega_9 \sum_{i<j} V(r_{ij}). \quad (58)$$

Since the helium-4 wave function is symmetric under the spatial exchange of any pair of nucleons, it follows that

$$W(R) = \frac{6}{\Omega_9} \int d\Omega_9 V(\sqrt{2}R\cos\theta) \quad (59)$$

or equivalently,

$$W(R) = \frac{315}{4} \int_0^1 dx (1-x^2)^2 x^2 V(\sqrt{2}Rx). \quad (60)$$

For the pair Coulomb potential,

$$V_C(r_{ij}) = \left(\frac{1}{2} + \tau_z(i)\right) \left(\frac{1}{2} + \tau_z(j)\right) \frac{e^2}{4\pi r_{ij}} \quad (61)$$

using the spin-isospin helium-4 wave function (52), the Coulomb potential can be reduced to

$$\begin{aligned} V_C(R) &= \sum_{i<j} \int d\Omega_9 \mathbf{P}^+(\sigma(i), \tau(i)) V_C(r_{ij}) \mathbf{P}(\sigma(i), \tau(i)) \\ &= \frac{35}{16\sqrt{2}R} \frac{e^2}{4\pi} = \frac{2.23 \text{ MeVfm}}{R}. \end{aligned} \quad (62)$$

We note the recent applications of this method to the clustering of light nuclei in heavy-ion collisions [36], and the charmed tetraquark states in [37].

Specific choices of the pair potential in Eq. (60) for helium-4 were discussed in [35,38,39]:

$$\begin{aligned} V_1(r) &= +144.86 e^{-(r/0.82)^2} - 83.34 e^{-(r/1.6)^2}, \\ V_2(r) &= +389.5 e^{-(r/0.7)^2} - 140.6 e^{-(r/1.4)^2} \end{aligned} \quad (63)$$

with the potential energy in MeV units, and the spatial range in fm. The above potentials are obtained by studying the binding energy of various light nuclei [38,39]. We have checked that the effect of the Coulomb interaction is negligible. The potentials in Eq. (63) capture schematically the repulsion at short distance (omega-exchange) and the attraction at large distance (pion-exchange). They reproduce the binding energy, electromagnetic radius, and the electromagnetic form factor of helium-4 up to momenta of the order of  $\frac{1}{2}m_N$  as detailed in Appendix A. This range can be extended to  $\frac{2}{3}m_N$  with our choice

$$V_3(r) = +1310.21 e^{-(r/0.7)^2} - 467.97 e^{-(r/1.16)^2}. \quad (64)$$

The reduced  $S$ -wave solutions to Eq. (56) for  $V_1$ ,  $V_2$ , and  $V_3$  are shown in Fig. 6 versus the hyperdistance. The binding energy of helium-4 with potential  $V_1$ ,  $V_2$ , and  $V_3$  are  $-27.75$  MeV,  $-28.47$  MeV, and  $-29.3$  MeV, respectively. The large induced centrifugation by projection on the hyperdistance causes it to peak at 2.5 fm. In the later sections, we will present the GFFs of helium-4 obtained with potential  $V_3$ .

## 2. Woods-Saxon potential (mean-field approximation)

For heavier nuclei the use of single particle states in the mean-field approximation is more convenient, modulo the center of mass motion. Although helium-4 does not qualify as a large nucleus, we will present the analysis for comparison with the  $K$ -harmonics method. In this case, the radial part of Eq. (43) will be sought using the independent particle states

$$\varphi[r_1, \dots, r_4] = \prod_{i=1}^4 \frac{u(r_i)}{r_i}. \quad (65)$$

The reduced  $u$  is solution to

$$u''(r) - \frac{m_N}{2\hbar^2}(E_H + V_{WS}(r))u(r) = 0 \quad (66)$$

in the Woods-Saxon potential

$$V_{WS}(r) = -\frac{V_0}{1 + e^{(r-R)/a}} \equiv -V_0 y(r) \quad (67)$$

and normalized as  $\int dr u^2 = 1$ . The depth  $V_0$ , range  $R$ , and skin  $a$  of the potential are fixed to reproduce helium-4 binding

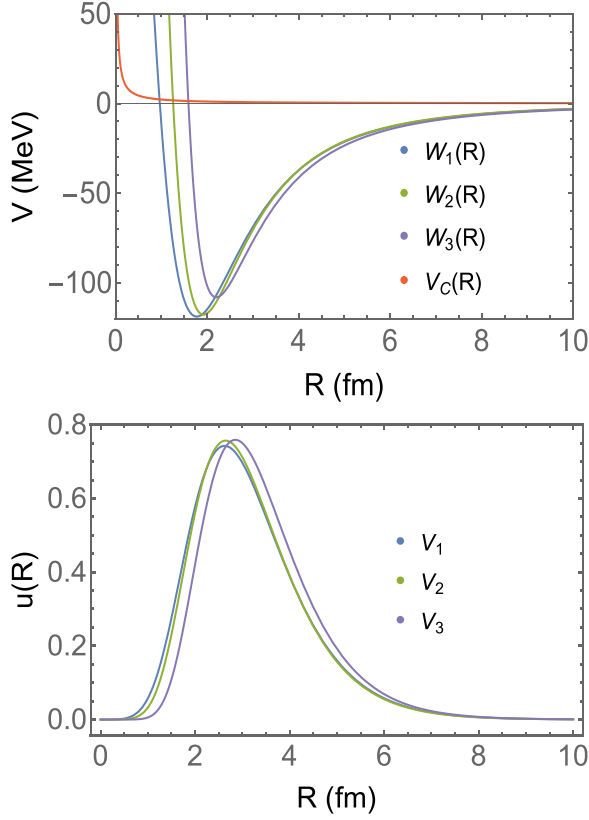


FIG. 6. Top: The potential  $W(R)$  and  $V_C(R)$  defined in Eqs. (60) and (62).  $W_1$ ,  $W_2$ , and  $W_3$  are obtained using  $V_1$ ,  $V_2$ , and  $V_3$  defined in Eqs. (63) and (64). Bottom: Helium-4  $S$  wave reduced wave function solution with potential  $V_1$ ,  $V_2$ , and  $V_3$  versus the hyperdistance.

energy per particle  $\frac{1}{4}E_H = 7.1$  MeV and radius  $r_H = 1.7$  fm. In general, the solution to Eq. (43) can be obtained in closed form, in terms of a generalized hypergeometric function [40]

$$u(r) = Cy(r)^\nu (1 - y(r))^\mu \times {}_2F_1(\mu + \nu, \mu + \nu + 1, 2\nu + 1, y(r)) \quad (68)$$

with  $C$  fixed by the normalization. Here, we have set  $\mu = i(\gamma^2 - \nu^2)^{\frac{1}{3}}$  and  $\nu > 0$  with

$$\nu^2 = \frac{a^2 E_H m_N}{2\hbar^2}, \quad \gamma^2 = \frac{a^2 V_0 m_N}{2\hbar^2}.$$

For light nuclei in general,  $V_0 = 50$  MeV,  $a = 0.51$  fm, and  $R = r_0 A^{\frac{1}{3}}$  with  $r_0 = 1.25$  fm.

In Fig. 7 we show the potential for  $A = 4$  (top), and the single particle state wave function for helium-4 (bottom). The numerical binding energy per particle is  $\frac{1}{4}E_H = 7.1$  MeV with a radius of 1.6 fm in agreement with the measured charge radius in [41].

### B. Helium-4 EMT

The way we have presented the derivation of the deuteron EMT results in the impulse approximation, can be applied verbatim to helium-4 using the wave function (43), with much simplifications and minor changes, thanks to the absence of

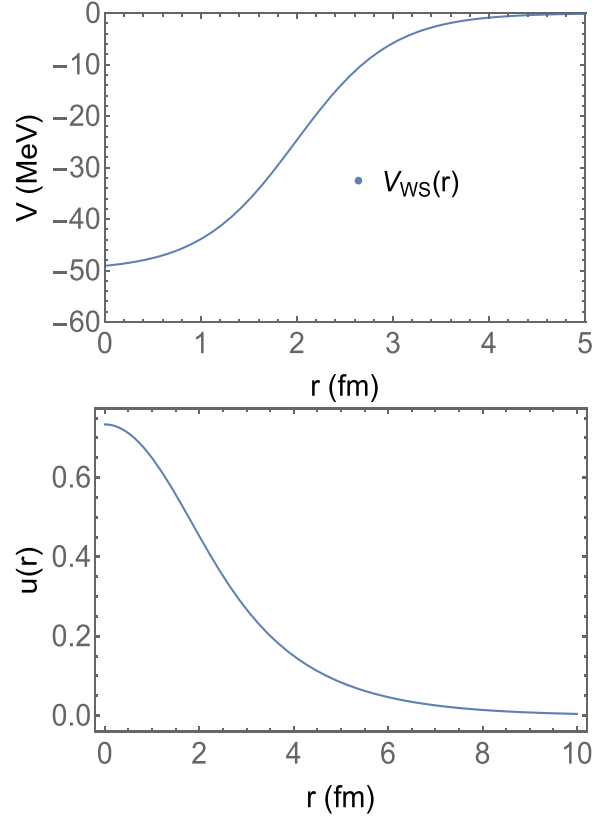


FIG. 7. Top: Woods-Saxon potentials  $V_{WS}$  for helium-4. Bottom: Helium-4  $S$  wave.

$D$ -wave admixture in helium-4. With this in mind, the results for helium-4 follow from Eq. (37) by inspection,

$$\begin{aligned} T_H^{00}(k) &= 4T_M(k)\bar{C}_E(k) \\ &= \left(m_\alpha + \frac{\vec{k}^2}{4m_\alpha}\right)A^H(k) + \frac{\vec{k}^2}{4m_\alpha}D^H(k), \\ T_H^{0j}(k) &= 0, \\ T_H^{jl}(k) &= 4C_M(k)\bar{C}_E(k) \frac{k^j k^l - \delta^{jl} \vec{k}^2}{m_N^2} \\ &= D^H(k) \frac{k^j k^l - \delta^{jl} \vec{k}^2}{4m_\alpha} \end{aligned} \quad (69)$$

with

$$\begin{aligned} A^H(k) &= \frac{4T_M(k)}{m_\alpha} \bar{C}_E(k) - \frac{\vec{k}^2}{m_\alpha^2} (T_M + 64C_M) \bar{C}_E(k) \\ &\approx A(k) \bar{C}_E(k), \end{aligned} \quad (70)$$

$$D_0^H(k) = 16 \frac{m_\alpha}{m_N^2} C_M(k) \bar{C}_E(k) \approx 64C(k) \bar{C}_E(k)$$

with the normalization  $\bar{C}_E(0) = 1$ .

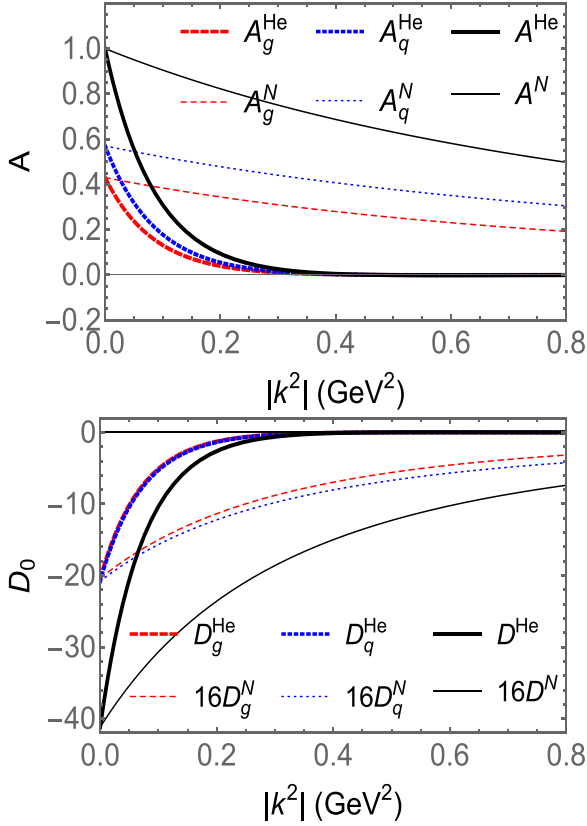


FIG. 8.  $A$ - and  $D$ -form factors for helium-4 obtained using  $K$ -harmonics method with potential  $V_3$ .

### 1. $K$ -harmonics

For the reduced S-wave solution (54) we have [35]

$$\begin{aligned}\bar{C}_E(k) &= \int dR d\Omega_9 \left( \frac{1}{4} \sum_{i=1}^4 e^{-ik \cdot (r_i - R_c)} \frac{|u(R)|^2}{\Omega_9} \right) \\ &= \int dR d\Omega_9 e^{i\frac{\sqrt{3}}{2} \vec{k} \cdot \vec{\xi}_3} \frac{|u(R)|^2}{\Omega_9} \\ &= 105 \int dR \frac{|u(R)|^2}{(\frac{1}{2}\sqrt{3}kR)^3} j_3\left(\frac{1}{2}\sqrt{3}kR\right),\end{aligned}\quad (71)$$

where we made use of the permutation symmetry of the helium-4 wave function expressed in Jacobi coordinates with  $\vec{r}_4 - \vec{R} = -\frac{\sqrt{3}}{2}\vec{\xi}_3$ .

### 2. Woods-Saxon potential

For the Woods-Saxon potential we have

$$\bar{C}_E(k) = \int_0^\infty u^2(r) j_0(kr) dr. \quad (72)$$

Note that  $kr$  instead of  $\frac{1}{2}kr$  appears in Eq. (72), as the reduced wave functions using the Woods-Saxon potential are coordinated from the center of mass.

In Fig. 8 we show the  $A$ ,  $D$  form factors for helium-4 using the  $K$ -harmonics method for the wave function with the spurious center of mass removed. In Fig. 9 we show the  $A$ ,  $D$  form

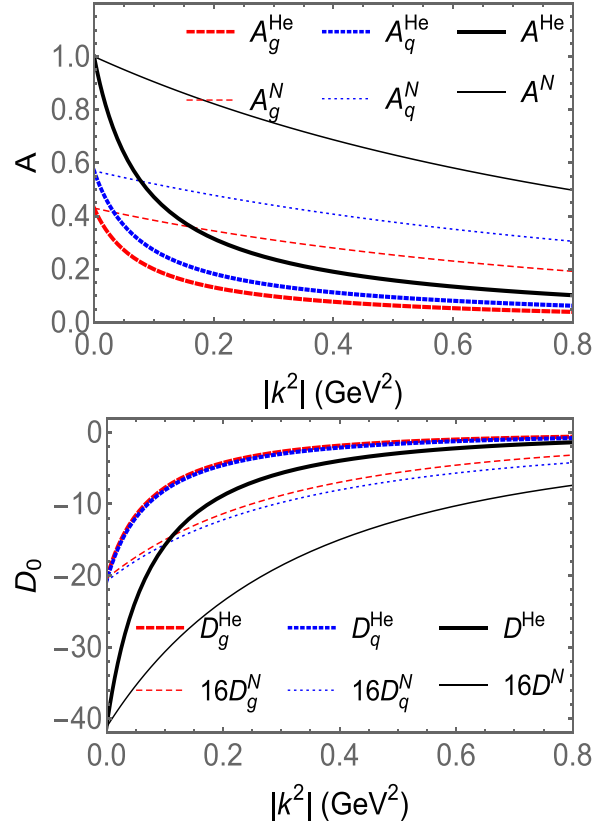


FIG. 9.  $A$ - and  $D$ -form factors for helium-4 obtained using a Woods-Saxon potential.

factors for helium-4, using the Woods-Saxon potential, without the removal of the spurious center of mass. The behavior of the form factors obtained with different approaches are quantitatively different in the intermediate momentum range with the  $A$ ,  $D$  form factors free of the center of mass motion, crossing the zero line at about  $k \sim m_N/2$ . The differences between the two constructions illustrate the importance of removing the center of mass motion, while describing the form factors for light nuclei. This point is further illustrated in our analysis of the charge form factors in Appendix A, where we note the agreement with the potential (64) up to  $\frac{2}{3}m_N$ , well within the range of validity of our nonrelativistic expansion. The gluon and quark contributions to the pressure  $p_{g,q}$  and shear  $s_{g,q}$  distributions are shown in Fig. 10, these results should be reasonable for distances  $r > 2\pi/(\frac{2}{3}m_N) \sim 2$  fm.

The results for helium-4, the lightest  $0^{++}$  magic nucleus, carry to heavier magic nuclei in the impulse approximation, with general  $A$  in the Woods-Saxon potential. In particular we have  $A^H(0) \approx A^0A(0) = 1$  and  $D^H(0) \approx A^2D(0)$  in the impulse approximation, which is to be compared to the scaling  $A^{\frac{7}{3}}$  suggested using a liquid drop model [6],  $A^{2.26}$  using relativistic nuclear potentials [7], and more recently  $A^{1.7-1.8}$  reported in the generalized Skyrme model [14]. In Fig. 11 we compare the  $D$ -form factor per nucleon, for the nucleon (red-solid line), deuteron (green-solid line), and helium-4 with  $K$ -harmonics method (black-solid line), and Woods-Saxon potential (blue-solid line).

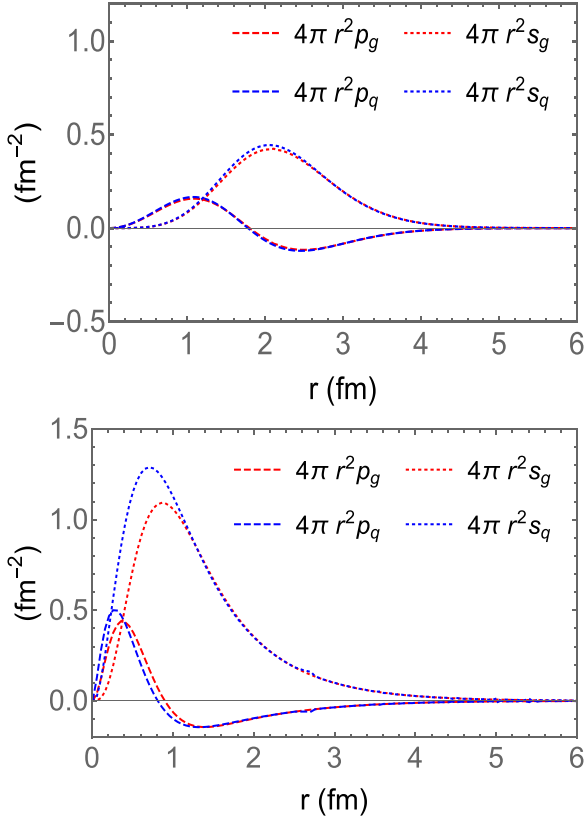


FIG. 10. The gluon and quark pressure  $p_{g,q}$  and shear  $s_{g,q}$  distributions in helium-4 using  $K$ -harmonics method (top) and Woods-Saxon potential (bottom), in the impulse approximation.

## VI. SCALAR AND MASS RADII

We now extend the proton definitions of the scalar radius  $r_S$  and the mass radius  $r_M$  to light nuclei, by defining the scalar and mass form factors

$$\mathbb{G}_S(k) = T^{00}(k) - T^{ii}(k), \quad \mathbb{G}_M(k) = T^{00}(k) \quad (73)$$

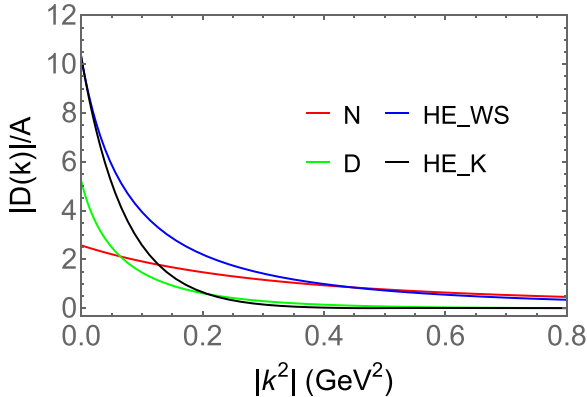


FIG. 11. The spin average  $D$  form factor normalized by the baryon number  $A$  in the nucleon ( $N$ ), deuteron ( $D$ ), and helium-4 ( $HE$ ) with sublabels for  $K$  harmonics with potentials  $V_3$  and Woods-Saxon.

for each of the deuteron and helium-4 with

$$r_{S,M}^2 = -6 \left( \frac{d \ln \mathbb{G}_{S,M}(k)}{d \bar{k}^2} \right)_{\bar{k}^2=0}. \quad (74)$$

The quark and gluon radii in light nuclei are presented in Table I, and compared to the charge radii following from Appendix A using the same wave functions. The quark and gluon separated radii in light nuclei are comparable, owing to the similarity of these radii in the nucleon following from Eq. (9). Overall, the difference between the scalar and mass radii seen in the nucleon, persists in light nuclei with the gluonic scalar radii larger than the mass radii, but both appear closer to the computed charge radii, in the impulse approximation. A similar observation was made in [15] for the light front transverse deuteron size, in the light cone convolution model.

## VII. CONCLUSIONS

We have analyzed the gravitational form factors for the deuteron in the context of the impulse approximation. The proton and neutron inside the deuteron were assumed nonrelativistic with the recoil of the spectator nucleon retained only to linear order. These approximations limit our gravitational form factors to momenta of the order of the nucleon mass.

The deuteron gravitational form factors  $A^D$ ,  $Q^D$ ,  $J^D$  capture the mass, quadrupole, and momentum distributions, supplemented by three additional  $D_0^D$ ,  $D_2^D$ ,  $D_3^D$  form factors reflecting on the standard tensor, spin-tensor, and mixed-spin-tensor contributions, respectively. Using the nucleon gravitational form factors, we have made explicit both the gluonic and fermionic contributions to each of the form factors. This budgeting reflects on the quantum delocalization of the concepts of quarks and gluons, in constituent bound states at low energy.

The deuteron scalar and mass radii from either the quarks or gluons are comparable to the deuteron electromagnetic radius. In contrast, the spin averaged quadrupole scalar and mass radii carried by the quarks and gluons are substantially smaller than the deuteron electromagnetic radius.

Our analysis of the deuteron, readily extends to helium-4, a much more compact nucleus. To describe the  $0^{++}$  ground state of helium-4, we have used both the  $K$ -harmonics method where the spurious center of mass motion is explicitly removed, and a Woods-Saxon potential with the spurious center of mass motion present. While the radii appears to be similar for both constructions, the ensuing form factors are substantially different, showing the importance of removing the spurious center of mass motion.

In the zero momentum limit, the mean-field approximation appears reliable in the determination of the mass radii, even with the unsubtracted center of mass motion. This observation allows for the extension of the mean-field approach to the heavier  $0^{++}$  magic nuclei  $O^{16}$ ,  $C^{40}$ , .... In particular, Eq. (69) can be extended to the heavier nuclei case, the spin average  $D$ -form factor for these heavier nuclei appears to scale as  $D^A(0) = A m_A / m_N D(0) \approx A^2 D(0)$  for a large atomic number  $A$ , in the impulse approximation. Although the nonrelativistic reduction holds in heavier nuclei, fermi motion requires

TABLE I. The quark and gluon EMT radii (fm) of light nuclei following from Eq. (73): scalar radii  $r_S$ , mass radii  $r_M$ ,  $r_{Q,S/M}$  spin averaged quadrupole radii, and  $r_E$  charge radii. For helium-4 we have listed the results from the  $K$  harmonics ( $K$ ) with potential  $V_3$  and Woods-Saxon potential (WS), with the bracketed results referring to experiment.

Nuclei	$r_S^g$	$r_S^q$	$r_M^g$	$r_M^q$	$r_{S,Q}^g$	$r_{S,Q}^q$	$r_{M,Q}^g$	$r_{M,Q}^q$	$r_E$
proton(experiment)	1.07 [2]	—	0.76 [2]	—	—	—	—	—	0.84 [42]
proton(input)	0.93 [22]	0.82	0.68 [22]	0.60	—	—	—	—	0.8
Deuteron	2.16	2.11	2.06	2.04	0.97	0.97	0.97	0.97	2.12 (2.13 [41])
Helium-4( $K$ )	1.80	1.76	1.69	1.67	—	—	—	—	1.79 (1.68 [43])
Helium-4(WS)	1.79	1.75	1.68	1.66	—	—	—	—	1.79 (1.68 [43])

that we include the next-to-leading order corrections in the spectator recoil. Also, exchange current corrections maybe important.

While our analysis has been considerably simplified by treating the light nuclei constituents nonrelativistically, limiting the range of the invariant form factors to about the nucleon mass, we plan to extend it to the relativistic case at least for the deuteron. Also, our analysis was limited to first order in the recoil of the struck nucleon or core. We plan to pursue the analysis to second order in the spectator recoil momentum, and investigate the importance of the exchange current contributions.

Our construction can be extended to analyze the generalized parton distributions (GPDs) for light nuclei, to understand the particular role played by the nucleon pair interaction, as well as exchange currents. Our gravitational form factors should prove useful for assessing diffractive photo- and electroproduction of heavy quarkonia on light nuclei.

The current effort at JLab to measure near threshold heavy quarkonia production on nucleons should be extended to light nuclei, to shed light on how the formation of nuclei may affect our understanding of mass and charge distributions, and the nature of the quantum delocalization of the quarks and gluons in bound states at low energy. Clearly, with the advent of the Electron-Ion Collider (EIC) with higher energy and luminosity, threshold photoproduction of quarkonia such as  $J/\Psi$ ,  $\Upsilon$  on light nuclei, should prove useful for addressing these issues.

## ACKNOWLEDGMENTS

We thank Zein-Eddine Meziani and Bao-Dong Sun for discussions. F.H. is supported by the National Science Foundation under CAREER Award No. PHY-1847893. I.Z. is supported by the Office of Science, U.S. Department of Energy under Contract No. DE-FG88ER40388. This research is also supported in part within the framework of the Quark-Gluon Tomography (QGT) Topical Collaboration, under Contract No. DE-SC0023646.

## APPENDIX A: LIGHT NUCLEI CHARGE FORM FACTORS

To compare the mass radii from the gravitational form factors to the charge radii for light nuclei, we provide here a simple estimate of their charge form factors, also in the impulse approximation. Since data are available, that allows us to gauge the validity of our method. With this in mind and

for a single nucleon, the electromagnetic current reads

$$J_N^\mu(k) = \bar{u}(p_2) e \left( F_1(k) \gamma^\mu + F_2(k) \frac{i\sigma^{\mu\nu} q_\nu}{2m_N} \right) u(p_1). \quad (\text{A1})$$

$F_1, F_2$  are the Dirac and Pauli form factors, which are related to the electric and magnetic Sachs form factors as

$$G_E(k) = F_1(k) - \frac{\vec{k}^2}{4m_N^2} F_2(k), \quad G_M(k) = F_1(k) + F_2(k), \quad (\text{A2})$$

The age-old Rosenbluth analysis of the electron scattering data up to 10 GeV<sup>2</sup> shows that the Sachs form factors for the proton are well approximated by dipoles

$$G_D(k) = \left( 1 + \frac{\vec{k}^2}{0.71} \right)^{-2}, \quad G_E^p(k) = G_D(k), \\ G_E^n(k) = 0, \quad G_M^{p,n}(k) = \mu_{p,n} G_D(k) \quad (\text{A3})$$

with the  $p, n$  empirical magnetic moments  $\mu_p = 2.79, -1.91$  (in Bohr magnetons). For completeness, we note that the JLab analysis based on the ratio of the polarization of the scattered proton shows  $G_E^p$  falling faster than  $G_M^p$  [44]:

$$G_E^p(k) = (1 - 0.13(\vec{k}^2 - 0.04)) G_D(k). \quad (\text{A4})$$

The leading nonrelativistic and recoil contributions to the nucleon charge form factor are

$$eJ_N^0(k) = e \left( G_E(k) + \frac{(\sigma \times ik) \cdot P}{4m_N^2} (2G_M(k) - G_E(k)) \right. \\ \left. + \mathcal{O}\left(\frac{\vec{k}^4}{m_N^4}, \frac{P^2}{m_N^2}\right) \right). \quad (\text{A5})$$

We now proceed to use Eq. (A5) for the modifications to the charge density in light nuclei, using the impulse approximation.

### 1. Deuteron charge form factor

Since the deuteron wave function is symmetric under spin exchange and independently space exchange of  $p, n$ , it follows that only the singlet combination of electric and magnetic form factors contribute to the deuteron charge form factor (A5) through the substitution

$$G_E^S(k) = \frac{G_E^p(k) + G_E^n(k)}{2}, \quad G_M^S(k) = \frac{G_M^p(k) + G_M^n(k)}{2} \quad (\text{A6})$$

with  $\sigma \rightarrow S$ . With this in mind, and using some of the matrix elements developed for the EMT form factors earlier, we obtain for the charge density in the impulse approximation

$$\begin{aligned} J_D^0(k, m', m) &= 2G_E^S(k) \left( C_E(k)\delta_{m'm} - 2C_Q(k)\langle m' | (S \cdot \hat{k})^2 - \frac{1}{3}S^2 | m \rangle \right) \\ &\quad - \frac{\vec{k}^2}{2m_N^2} (2G_M^S(k) - G_E^S(k)) (D_0^{SP}(k)\delta_{m'm} + (D_2^{SP}(k) + 2D_3^{SP}(k))\langle m' | Q^{ij}\hat{k}^i\hat{k}^j | m \rangle) \\ &= F_C^D(k)\delta_{m'm} + F_Q^D(k)\frac{k^\alpha k^\beta}{2m_D^2}\langle m' | Q^{\alpha\beta} | m \rangle. \end{aligned} \quad (\text{A7})$$

The squared electric charge radius of the deuteron is the sum of the nucleon, plus the intrinsic  $C_E$ -form factor contribution

$$\langle r^2 \rangle_D = \langle r^2 \rangle_N + \langle r^2 \rangle_{C_E}. \quad (\text{A8})$$

The results for the electric charge form factor for the deuteron  $|F_C^D|$  in Eq. (A7) are shown in Fig. 12 (top), and compared to the empirical data in [45]. The impulse approximation works reasonably well in this momentum range, although the diffractive

dip is slightly off to the right of the empirical values. The diffractive pattern with a first zero at about  $k_D^2 \approx 0.75 \text{ GeV}^2$ , reflects on the good deuteron  $S$ -wave function from the soft Reid potential in Fig. 1, with a peak at  $a_D \approx 1.5 \text{ fm}$  (diffraction disk size).

## 2. Helium-4 charge form factor

For helium-4, the charge density in the impulse approximation reads

$$J_{He}^0(k) = 4G_E^S(k)\bar{C}_E(k) = 2F_C^{He}(k), \quad (\text{A9})$$

where the analog of the singlet substitution (A6) applies, because of the spin and space symmetry of the underlying wave function. Note that at low momentum transfer Eq. (A9) simplifies to

$$F_C^{He}(k) \approx F_C^D(k). \quad (\text{A10})$$

The squared electric charge radius of helium-4 is the sum of the nucleon plus the intrinsic  $\bar{C}_E$  form factor contribution

$$\langle r^2 \rangle_H = \langle r^2 \rangle_N + \langle r^2 \rangle_{\bar{C}_E}. \quad (\text{A11})$$

The results for the electric charge form factor for helium-4  $|F_C^{He}|$  in Eq. (A9) are shown in Fig. 12 (bottom) for the Woods-Saxon potential (red-triangle) and the  $K$  harmonics with potential  $V_1$  (dotted-blue line),  $V_2$  (green diamond)  $V_3$  (purple triangle), and compared to the empirical data (yellow square) in [47]. Note that the diffractive minima following from  $V_1$ – $V_3$  are different. The corresponding wave functions shown in Fig. 6 are similar but not identical, especially in the small  $R$  region, which is at the origin of the difference in the  $k > m_N/2$  region. The result with Woods-Saxon potential does not display a diffraction pattern, since the single-particle wave function in Fig. 7 shows no plateau or disk. The  $K$  harmonics does, and the discrepancy between the measured diffractive minimum and the  $K$ -harmonics minimum, could be narrowed by optimizing the potential choice in Eq. (63). Away from the diffractive minima, the  $K$ -harmonics electric form factor and the measured one are comparable in magnitude.

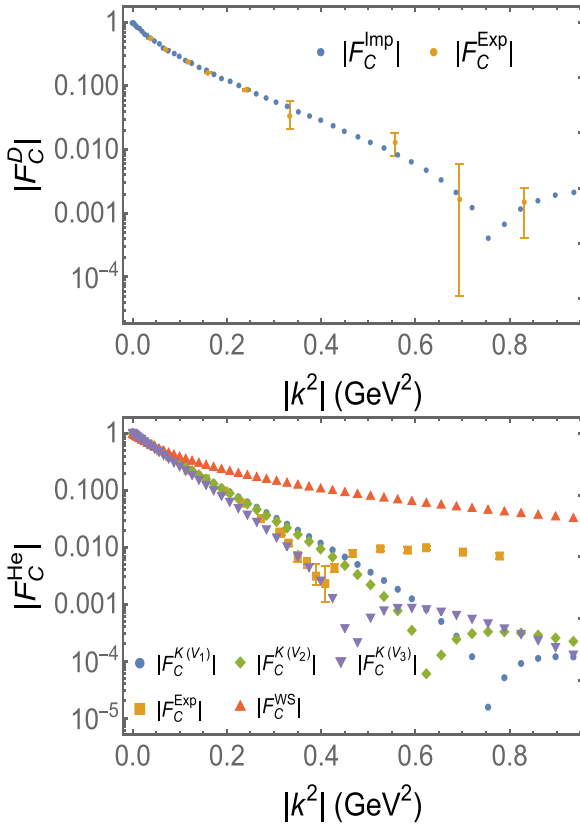


FIG. 12. Top: Deuteron electric charge form factors in the impulse approximation compared to experiment [46]. Bottom: Helium-4 electric charge form factors using the  $K$ -harmonics method with the potentials in Eqs. (63) and (64) and the Woods-Saxon potential, compared to experiment [47].

## APPENDIX B: PRESSURE AND SHEAR FORCE

Following [31], the stress tensor defined by the  $ij$  components of the EMT is defined as ( $a = q, g$ ),

$$\begin{aligned}
 T_a^{jl}(\vec{r}, m', m) &= \int \frac{d^3k}{(2\pi)^3} \frac{m_D}{E} e^{-ik \cdot r} \left\langle +\frac{k}{2} m' \left| \hat{T}_a^{jl}(0) \right| -\frac{k}{2} m \right\rangle \\
 &= (p_0(r)\delta^{jl} + s_0(r)Y_2^{jl})\delta_{m'm} + p_2(r)\langle m' | Q^{ij} | m \rangle \\
 &\quad + 2s_2(r)\langle m' | \hat{Q}^{lp} Y_2^{pj} + \hat{Q}^{jp} Y_2^{pl} \\
 &\quad - \delta^{jl} \hat{Q}^{pq} Y_2^{pq} | m \rangle \\
 &\quad + \langle m' | Q^{\alpha\beta} | m \rangle \hat{\delta}_\alpha \hat{\delta}_\beta [p_3(r)\delta^{jl} + s_3(r)Y_2^{jl}]
 \end{aligned} \tag{B1}$$

with  $Y_2^{jl} = \hat{r}^l \hat{r}^j - \frac{1}{3}\delta^{jl}$ . The pressure and shear force follow as

$$\begin{aligned}
 p_i &= \frac{1}{3} \frac{1}{r^2} \frac{d}{dr} r^2 \frac{d}{dr} \tilde{D}_i(r), \\
 s_i &= -\frac{1}{2} r \frac{d}{dr} \frac{1}{r} \frac{d}{dr} \tilde{D}_i(r).
 \end{aligned} \tag{B2}$$

Here,  $\tilde{D}_i$  are the Fourier transform of the deuteron form factors  $D_i$  defined in Eq. (37),

$$\tilde{D}_{0,2,3}(r) = \int \frac{d^3k}{2E(2\pi)^3} e^{-ik \cdot r} D_{0,2,3}(k). \tag{B3}$$

For helium-4 without the small  $D$ -wave admixture, the pressure and shear force receive contribution only from  $D_0$ .

- 
- [1] A. Ali *et al.* (GlueX Collaboration), *Phys. Rev. Lett.* **123**, 072001 (2019).
- [2] B. Duran *et al.*, *Nature (London)* **615**, 813 (2023).
- [3] T. W. Donnelly and J. D. Walecka, *Annu. Rev. Nucl. Sci.* **25**, 329 (1975).
- [4] D. O. Riska, *Phys. Rep.* **181**, 207 (1989).
- [5] G. E. Brown and A. D. Jackson, *The Nucleon-Nucleon Interaction* (North-Holland, 1976).
- [6] M. V. Polyakov, *Phys. Lett. B* **555**, 57 (2003).
- [7] V. Guzey and M. Siddikov, *J. Phys. G* **32**, 251 (2006).
- [8] H.-C. Kim, P. Schweitzer, and U. Yakhshiev, *Phys. Lett. B* **718**, 625 (2012).
- [9] J. Hudson and P. Schweitzer, *Phys. Rev. D* **96**, 114013 (2017).
- [10] R. Dupré and S. Scopetta, *Eur. Phys. J. A* **52**, 159 (2016).
- [11] Y. Dong and C. Liang, *Nucl. Phys. A* **918**, 25 (2013).
- [12] S. Scopetta, *Phys. Rev. C* **70**, 015205 (2004).
- [13] S. Scopetta, *Nucl. Phys. A* **755**, 523 (2005).
- [14] A. G. Martin-Caro, M. Huidobro, and Y. Hatta, *Phys. Rev. D* **108**, 034014 (2023).
- [15] A. Freese and W. Cosyn, *Phys. Rev. D* **106**, 114013 (2022).
- [16] R. Wang, C. Han, and X. Chen, *Phys. Rev. C* **109**, L012201 (2024).
- [17] R. V. Reid, Jr., *Ann. Phys.* **50**, 411 (1968).
- [18] H. Pagels, *Phys. Rev.* **144**, 1250 (1966).
- [19] P. Carruthers, *Phys. Rev. D* **2**, 2265 (1970).
- [20] M. V. Polyakov and P. Schweitzer, *Int. J. Mod. Phys. A* **33**, 1830025 (2018).
- [21] D. C. Hackett, D. A. Pefkou, and P. E. Shanahan, *arXiv:2310.08484* [hep-lat].
- [22] K. A. Mamo and I. Zahed, *Phys. Rev. D* **106**, 086004 (2022).
- [23] Y. Guo, X. Ji, M. G. Santiago, K. Shiells, and J. Yang, *J. High Energy Phys.* **05** (2023) 150.
- [24] D. E. Kharzeev, *Phys. Rev. D* **104**, 054015 (2021).
- [25] X. Ji, *Front. Phys.* **16**, 64601 (2021).
- [26] Y. Hatta and M. Strikman, *Phys. Lett. B* **817**, 136295 (2021).
- [27] Y. Guo, X. Ji, and Y. Liu, *Phys. Rev. D* **103**, 096010 (2021).
- [28] P. Sun, X.-B. Tong, and F. Yuan, *Phys. Lett. B* **822**, 136655 (2021).
- [29] X.-Y. Wang, F. Zeng, and Q. Wang, *Phys. Rev. D* **105**, 096033 (2022).
- [30] F. Gross, *Phys. Rev.* **140**, B410 (1965).
- [31] M. V. Polyakov and B.-D. Sun, *Phys. Rev. D* **100**, 036003 (2019).
- [32] A. M. Badalian and Y. A. Simonov, *Sov. J. Nucl. Phys.* **3**, 755 (1966).
- [33] M. F. de La Ripelle and J. Navarro, *Ann. Phys.* **123**, 185 (1979).
- [34] F. D. Santos, S. A. Tonsfelt, T. B. Clegg, E. J. Ludwig, Y. Tagishi, and J. F. Wilkerson, *Phys. Rev. C* **25**, 3243 (1982).
- [35] J. Castilho Alcaras and B. Pimentel Escobar, *Revista Brasileira de Física* **4**, 83 (1974).
- [36] E. Shuryak and J. M. Torres-Rincon, *Phys. Rev. C* **101**, 034914 (2020).
- [37] N. Miesch, E. Shuryak, and I. Zahed, *Phys. Rev. D* **109**, 014022 (2024).
- [38] A. Volkov, *Nucl. Phys.* **74**, 33 (1965).
- [39] D. M. Brink and E. Boeker, *Nucl. Phys. A* **91**, 1 (1967).
- [40] S. Flügge and W. Franzen, *Phys. Today* **29**, 55 (1976).
- [41] M. Kalinowski, *Phys. Rev. A* **99**, 030501(R) (2019).
- [42] R. L. Workman *et al.* (Particle Data Group), *PTEP* **2022**, 083C01 (2022).
- [43] I. Sick, *Phys. Rev. C* **77**, 041302(R) (2008).
- [44] O. Gayou *et al.* (Jefferson Lab Hall A Collaboration), *Phys. Rev. Lett.* **88**, 092301 (2002).
- [45] A. Bekzhanov, S. Bondarenko, and V. Burov, *Nucl. Phys. B* **245**, 65 (2013).
- [46] M. Garcon *et al.*, *Phys. Rev. C* **49**, 2516 (1994).
- [47] R. F. Frosch, J. S. McCarthy, R. e. Rand, and M. R. Yearian, *Phys. Rev.* **160**, 874 (1967).